ACADEMIC PRESS

Elucidation of sulfidation state and hydrodesulfurization mechanism on ruthenium–cesium sulfide catalysts using ^{35}S radioisotope tracer methods

Atsushi Ishihara,* Jeayoung Lee, Franck Dumeignil, Ryuichirou Higashi, Anjie Wang, Eika W. Qian, and Toshiaki Kabe

Department of Chemical Engineering, Tokyo University of Agriculture & Technology, Nakacho, Koganei, Tokyo 184-8588, Japan

Abstract

Alumina-supported ruthenium–cesium catalysts were presulfided using $[^{35}S]H_2S$ pulse tracer method to evaluate their sulfidation state. Subsequently, using these previously ^{35}S-labeled catalysts, HDS reactions of dibenzothiophene (DBT) were performed and the mobility of ^{35}S introduced during the presulfidation stage was investigated. The results showed that the amount of labile sulfur (S_0) was much smaller than the total amount of sulfur accommodated on the catalyst (S_{total}). DBT conversion and S_{total} increased linearly with Ru content. In a second part, labile sulfur amount was also determined under the catalyst working conditions and different results were obtained. Indeed, when the catalysts were marked with $[^{35}S]$ and with $[^{35}S]DBT$ under HDS reaction conditions, the obtained labile sulfur quantities (S_{0A}) were significantly higher than the ones measured during the presulfidation stage (S_0). These results showed that the labile sulfur is not formed on RuCs catalysts until the HDS reaction proceeds, which is quite different from that reported before for Mo, Pt, or Pd systems.
© 2003 Elsevier Science (USA). All rights reserved.

Keywords: Hydrodesulfurization; Dibenzothiophene; ^{35}S; Radioisotope; Tracer; Ruthenium; Cesium; Sulfide; Alumina

1. Introduction

In big city areas the problem of air pollution due to diesel engine fumes has become more and more serious. Therefore, a number of approaches aiming at performing deep hydrodesulfurization (HDS) of light gas oils have been investigated. For deep HDS reactions, the development of very efficient new HDS catalysts, with knowledge of the active phase as well as the HDS reaction mechanism [1] is needed.

Among a large number of attempts, much attention has been focused on unsupported ruthenium sulfides, which were found to be the most active in the hydrodesulfurization of thiophenes using transition metal sulfides [2–6]. Some research groups have performed HDS reactions catalyzed by ruthenium sulfide supported on alumina [7–10] carbon [11–13], zeolites, [14–18], MgF$_2$, [19], and amorphous silica–alumina [20]. However, supported ruthenium sulfide activity was not always so high [8]. Preparation conditions were found to play an important role in the activity,

and the catalysts derived from supported metal carbonyls showed a catalytic activity higher than that of conventionally prepared catalysts [21,22], which was also observed by some authors of the present paper [10,23]. Furthermore, cesium hydroxide addition during the preparation ruthenium carbonyl-based catalysts showed a remarkable increase in catalytic activity [24–27].

For more conventional catalysts, the necessity and/or influence of presulfiding parameters has been extensively reported [28,29]. Using conventional investigation methods, oxidation states before and after presulfiding can be obtained. However, catalyst sulfidation state is very unstable, and it appears necessary to investigate the working catalyst in situ to obtain reliable structural information. Therefore, in order to clarify the sulfur behavior on the working catalysts during practical HDS conditions, ^{35}S radioisotope tracer methods were developed, giving access to quantitative data [30–53]. In the present paper, ^{35}S radioisotope tracer methods were used to study the particular case of Ru-based HDS catalysts. Indeed, under a H$_2$ atmosphere it is known that sulfided Ru species can be reduced (giving H$_2$S release), and a decrease in HDS activity is observed. Ru-based HDS catalyst sulfidation state is therefore

---

* Corresponding author.
  E-mail address: atsushii@cc.tuat.ac.jp (A. Ishihara).

a sensitive parameter which can vary under different experimental conditions. We decided therefore to check the difference between the sulfidation state after the presulfidation stage and the sulfidation state of the working catalysts. For this purpose two different experimental methods were carried out. In the first one, catalysts were presulfided using $[^{35}S]H_2S$ and sulfidation state was estimated quantitatively (quantity of accommodated sulfur). Then, using the obtained ^{35}S-labeled catalysts, the HDS reaction of DBT was performed to estimate the amount of labile sulfur generated under the presulfidation conditions (i.e., determination of released $[^{35}S]H_2S$ quantity during the DBT HDS reaction). In the second experimental procedure, DBT HDS reactions of ^{35}S-labeled DBT (equivalent to a labeling of the active sites directly with $[^{35}S]DBT$) were carried out on the catalysts and the amount of labile sulfur was obtained by quantifying the released $[^{35}S]H_2S$ quantity when feed was changed to $[^{32}S]DBT$. Labile sulfur quantities obtained by both methods were compared, and the obtained differences were discussed. Further, results were compared with those previously obtained for Mo, Pt, and Pd-based catalysts [52,54].

2. Experimental section

2.1. Preparation of catalysts

Ruthenium carbonyl and cesium hydroxide were purchased from Kishida Chemicals Co., Ltd., and γ-Al$_2$O$_3$ was supplied from Nippon Ketjen Co., Ltd. γ-Al$_2$O$_3$ was crushed to 20–30 mesh prior to use. An anionic ruthenium carbonyl complex was prepared by reaction of Ru$_3$(CO)$_{12}$ with an excess of CsOH in methanol using Cs/Ru = 1–3. It is well known that Ru$_3$(CO)$_{12}$ reacts with alkali metal hydroxides to give anionic ruthenium hydride complexes [25] M[HRu$_3$(CO)$_{11}$] with M = Cs in the present paper. Then, alumina was added into the prepared {Cs[HRu$_3$(CO)$_{11}$] + unreacted CsOH} solution. After the mixture was stirred for 2 h, the solvent was removed in vacuo. Various catalysts were prepared by variation of the metal loading. First, Ru content was varied from 4 to 20 wt% keeping the Ru + alumina weight equal to 1 g, and Cs/Ru = 1. A second series of catalysts was prepared by fixing the Ru loading at 8 wt% and varying the Cs/Ru ratio from 0 to 3. Because the prepared catalysts are unstable under atmospheric conditions, they were prepared and stored under argon atmosphere.

2.2. Synthesis of $[^{35}S]H_2S$

^{35}S-labeled hydrogen sulfide ($[^{35}S]H_2S$) was prepared as follows.

First, ^{32}S and ^{35}S were added into a crucible, to obtain a total radioactivity of 4 MBq and total weight of 7 g.

Subsequently, the crucible was charged into an autoclave (Nittoh Kouatsu Co., Ltd., 367 mL). After H$_2$ purge, the autoclave was pressurized with H$_2$ to 50 kg/cm^2 and heated at 430 °C, and this temperature was kept for 1 h.

After cooling to room temperature, the autoclave was further cooled into liquid nitrogen to solidify $[^{35}S]H_2S$. Unreacted hydrogen was then completely removed using a vacuum pump and 100% gaseous $[^{35}S]H_2S$ was collected by returning the autoclave to room temperature. Then, by adding hydrogen in a proper quantity, the mixed gas used for the presulfiding experiments (about 30% of H$_2$S in H$_2$) was prepared. Accurate gas concentration was measured by using a GC-TCD apparatus (Hitachi 263) equipped with a Porapack Q column (length, 3 m; id, 3 mm). Column, injection, and detector temperatures were set to 180, 200, and 200 °C, respectively.

2.3. Measurement of surface area, pore volume, and pore distribution

0.1 g of presulfided sample was weighted and then charged into the BET apparatus (Coulter Co. SA3100). After outgassing at 200 °C for 2 h, a 10-point BET method measurement was performed. The pore distribution was obtained using the BJH method [55].

Table 1 shows the surface area and the pore volume of the catalysts. For the catalysts with Cs/Ru ratio equal to 1, when the Ru content was gradually increased from 4 to 20 wt%, specific surface area decreased from 246 to 144 m^2/g. Pore volume was quite constant for 4–8 Ru wt% but decreased for higher Ru loading. Fig. 1 shows pore distribution curves. Mean pore radius was found to be around 40 Å for all the catalysts. Therefore, pore radius variation was not a parameter that could explain the variations of DBT HDS activity over the catalysts.

Catalysts with various Cs/Ru ratios exhibited a decrease in pore volume and specific surface area (see the bottom of Table 1). Fig. 2 shows the pore distribution curves for the catalysts with Cs/Ru = 0–3. Mean pore radius was also found to be about 40 Å for all the catalysts.

Table 1
BET surface area and pore volume of the catalysts

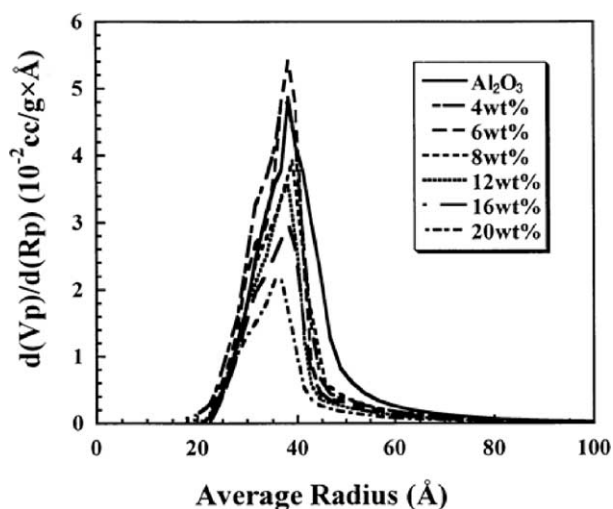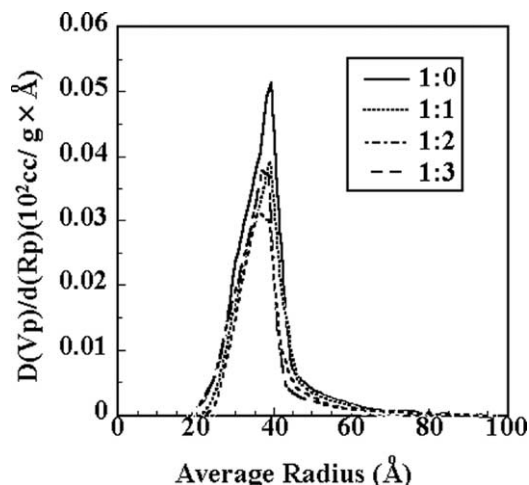| Ruthenium content (wt%)	Cs/Ru ratio (mol/mol)	Surface area (m^2/g)	Pore volume (cm^3/g)
0 (alumina)	–	256	0.647
4	1	246	0.494
6	1	245	0.549
8	1	210	0.489
12	1	188	0.400
16	1	158	0.358
20	1	144	0.279
8	0	250	0.609
8	2	169	0.430
8	3	146	0.247

Fig. 1. Pore distribution of Ru–Cs/Al$_2$O$_3$ catalysts.

Fig. 2. Pore distribution of Ru–Cs/Al$_2$O$_3$ catalysts.

2.4. Determination of (pre)sulfidation state of Ru–Cs catalysts using [^{35}S]H$_2$S radioisotope pulse tracer method

A pressurized fixed-bed flow reactor was used for pre-sulfiding experiments. Fig. 3 shows the reaction apparatus used for the [^{35}S]H$_2$S pulse tracer method. 0.5 g of catalyst was packed into the reactor. The mixed gas (30% [^{35}S]H$_2$S/H$_2$) was charged into a 5.04 cm^3 loop line. By using a 6-way valve, [^{35}S]H$_2$S/H$_2$ mixed gas was periodically introduced into the reactor kept under a flow of N$_2$ carrier gas (50 kg/cm^2, 5 L/h) at 100, 200, and 300 °C. After each pulse, the unreacted [^{35}S]H$_2$S/H$_2$ was collected in a trap placed at the outlet of the reactor (absorption into 10 mL of a basic Carbosorb scintillation solution). The amount of collected radioactivity after each pulse was then measured by using a liquid scintillation counter. This operation was repeated until the amount of radioactivity in a recovered pulse

became equal to the introduced one (steady state), i.e., when S uptake on the studied catalyst reached saturation. After the presulfiding experiment, a liquid-gas separator was installed under the reactor tube, and the DBT HDS reaction was carried out using the following parameters: 300 °C, total pressure = 50 kg/cm^2, WHSV = 28 h^{-1}, hydrogen flow rate = 12.5 L/h, with a 1 wt% DBT solution in decalin. Reaction products in the liquid phase were analyzed by GC-FID.

2.5. Hydrodesulfurization of [^{35}S]DBT on Ru–Cs catalysts

The [^{35}S]DBT HDS experimental procedure used in this paper has been already described elsewhere [49] but we will give a brief description of it in order to make the experimental results easier to interpret for the reader. HDS of [^{35}S]DBT was carried out in a pressurized flow reactor, and typical reaction conditions were fixed as follows: 300 °C,
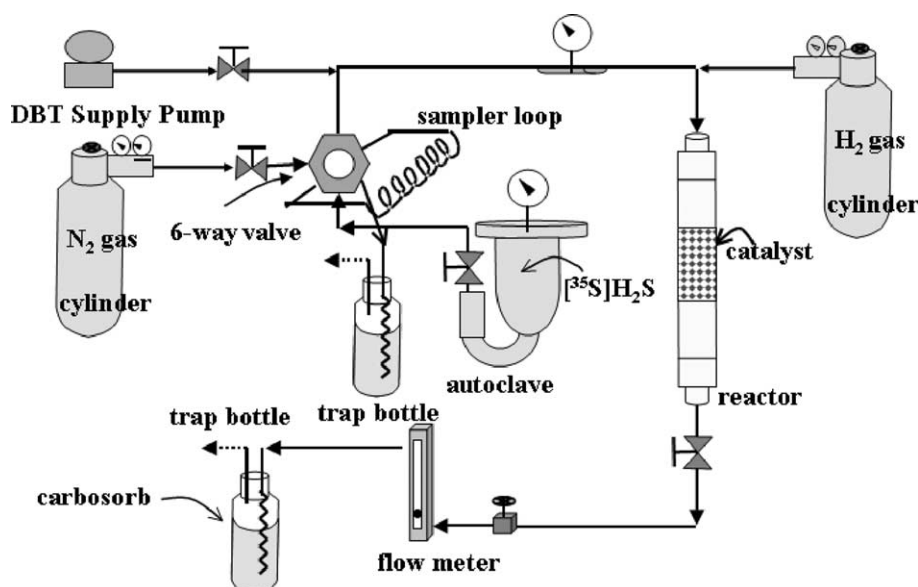

Fig. 3. Experimental apparatus of ^{35}S pulse tracer method.

total pressure = 50 kg/cm^2, WHSV = 28 h^{-1}, hydrogen flow rate = 25 L/h, with a 1 wt% DBT solution in decalin. The catalysts were presulfided with a 3 vol% H$_2$S/H$_2$ gas mixture at 300 °C during 3 h. In a first step, the HDS reaction of DBT was carried out using a 1 wt% [^{32}S]DBT solution in decalin during 3 h. Then, when the conversion of DBT became constant, [^{32}S]DBT was replaced by 1 wt% [^{35}S]DBT and the reaction was pursued for 4–7 h (HDS sites labeling with [^{35}S]). Then, decalin solution was introduced into the reactor for 3 h and the HDS reaction using [^{32}S]DBT was performed again for 4–7 h. [^{35}S]H$_2$S produced during this last reaction was absorbed in a basic scintillator solution and liquid products were analyzed in the same way as described in [54]. The radioactivities of both unreacted [^{35}S]DBT and formed [^{35}S]H$_2$S were measured with a liquid scintillation counter (Beckman LS-6500, Beckman Co., Ltd.) after a proper scintillation solvent (Permafluor or Instafluor, Packard Japan Co., Ltd.) was added to each sampled fraction. The liquid scintillation counting method was explained in another paper [56] and detailed calculation methods for accommodated sulfur quantity and labile sulfur quantity are also given elsewhere [49].

3. Results and discussion

3.1. Sulfur quantitative analysis of the presulfided Ru–Cs catalysts by a ^{35}S radioisotope pulse tracer method

Fig. 4 shows the changes in recovered radioactivity after each [^{35}S]H$_2$S pulse introduction. Each box on the graph represents the radioactivity of [^{35}S]H$_2$S released from the reactor after each pulse. The shaded part represents therefore the radioactivity of sulfur incorporated into the catalyst. Then, the total amount of sulfur (S_{total}) accommodated at each temperature can be easily deduced.
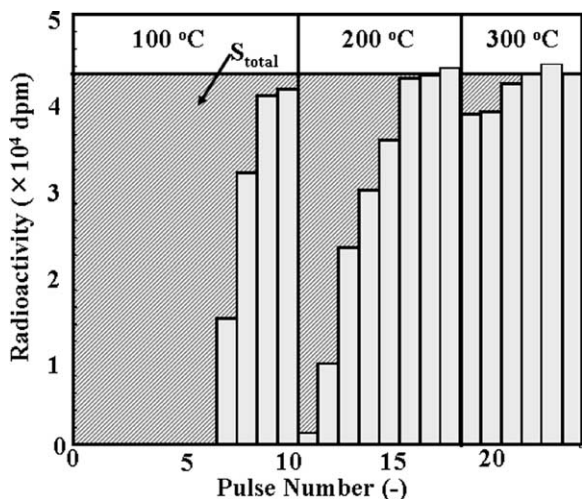
Catalysts presulfided with [^{35}S]H$_2$S by the method described above were purged with decalin (further used as a solvent for the reactant feed) before introduction of the 1 wt% DBT solution. The amount of radioactivity released from the catalyst (in the liquid and the solid phase) was followed during the HDS reaction. The radioactivity of ^{35}S detected during the purge with decalin was attributed to the evacuation of physisorbed [^{35}S]H$_2$S species which dissolved in the solvent. The physisorbed H$_2$S quantity was found to be very small when compared to the accommodated sulfur total quantity. However, we decided to subtract it from the calculated accommodated sulfur quantity to calculate accurately S_{total}, which represented therefore the total *chemisorbed S* quantity present on the catalyst surface after presulfidation. Then, when DBT solution was introduced under a pressurized hydrogen atmosphere, the HDS reaction was followed by ^{35}S detection in both liquid and gas phases (Fig. 5). Released radioactivity was regarded as the labile sulfur created during the presulfidation step (S_0). Obtained S_0 values were surprisingly much smaller than the total amount of sulfur incorporated during the presulfiding step. That means that only a very little amount of labile sulfur was created during the presulfidation step. The global results are given in Figs. 6 and 7 and in Table 2. The conversion of DBT and the amount of sulfur accommodated on the catalyst (S_{total}) as well as S_0 increased linearly with increasing Ru content (Fig. 6). As a remark, it is well-known that Ru can be sulfided into RuS$_2$, that means that Ru on the catalysts was only sulfided up to about 50% during the presulfidation stage.

The effect of Cs on Ru sulfidation state was checked. In a first part, we decided to check Cs–alumina solids. We prepared a series of Cs/Al$_2$O$_3$ catalysts and presulfiding [^{35}S]H$_2$S experiments were performed as described above. Fig. 8 shows the variation of the total amount of sulfur accommodated on the catalysts with Cs content. With increasing Cs content, the total amount of sulfur (S_{total}) incorporated into Cs/Al$_2$O$_3$ catalysts increased linearly in
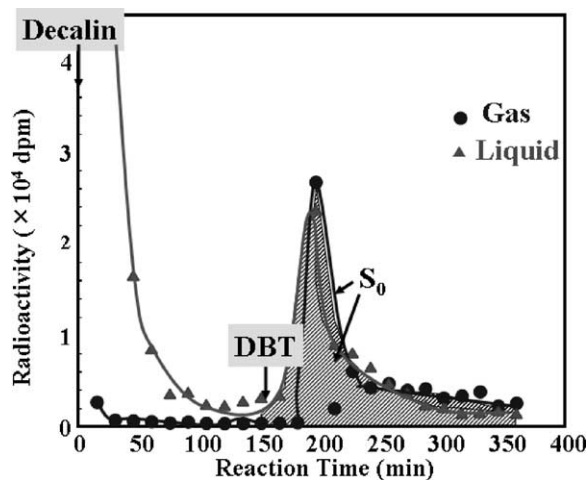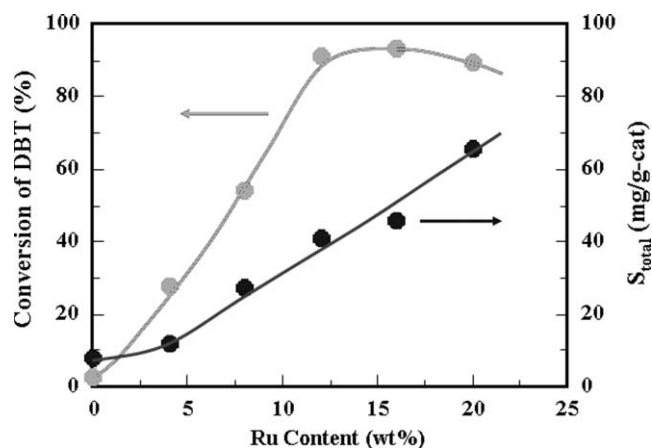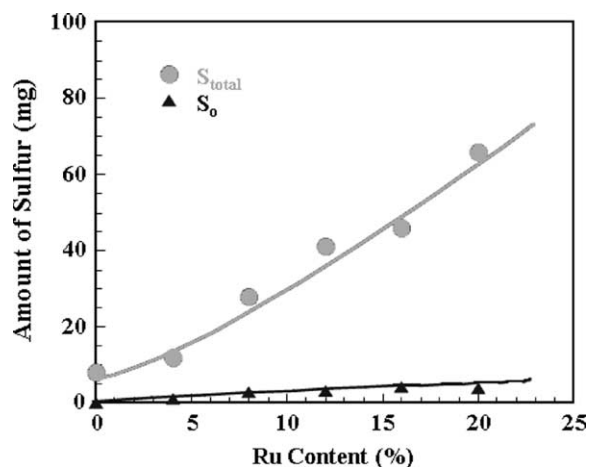

Fig. 4. Sulfidation of 8 wt% Ru–Cs/Al$_2$O$_3$ with [^{35}S]H$_2$S pulses (Ru:Cs = 1:3).

Fig. 5. Changes in radioactivity of ^{35}S with reaction time (8 wt% Ru–Cs/ Al$_2$O$_3$ (Ru:Cs = 1:3)).

Fig. 6. Effect of Ru content on DBT conversion and S_{total}.

Fig. 7. Change in amount of sulfur with Ru content in Ru–Cs/Al$_2$O$_3$ catalysts (Ru/Cs = 1).

parallel with the one observed for Ru–Cs/Al$_2$O$_3$ catalysts. It was observed that approximately 60–82% of the total amount of sulfur accommodated on Ru–Cs/Al$_2$O$_3$ catalysts was equivalent to S_{total} of Cs/Al$_2$O$_3$ catalysts (for the same Cs loading). That means that a considerable amount of S_{total} in the Ru–Cs/Al$_2$O$_3$ catalysts was linked to the presence of Cs in the system.
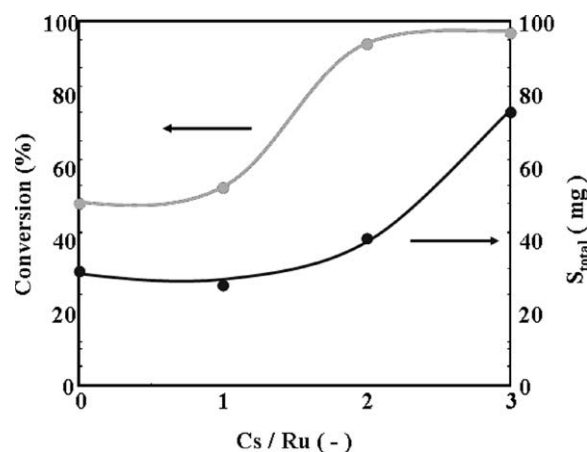
Table 2
Kinetic parameters on Ru–Cs/Al$_2$O$_3$

Ru (wt%)	Conversion (%)	S_{total} (mg/g-cat)	S_0 (mg/g-cat)	S_{0A} (mg/g-cat)
4	28	12 (RuS$_{0.94}$)	1.0	7.3 (RuS$_{057}$)
8	54	28 (RnS$_{1.11}$)	2.8	12.9 (RuS$_{0.51}$)
12	91	41 (RuS$_{1.08}$)	3.3	20.8 (RuS$_{0.55}$)
16	94	46 (RuS$_{0.91}$)	4.3	37.9 (RuS$_{0.75}$)
20	89	66 (RuS$_{1.04}$)	3.7	45.0 (RuS$_{0.71}$)

(Ru/Cs = 1).
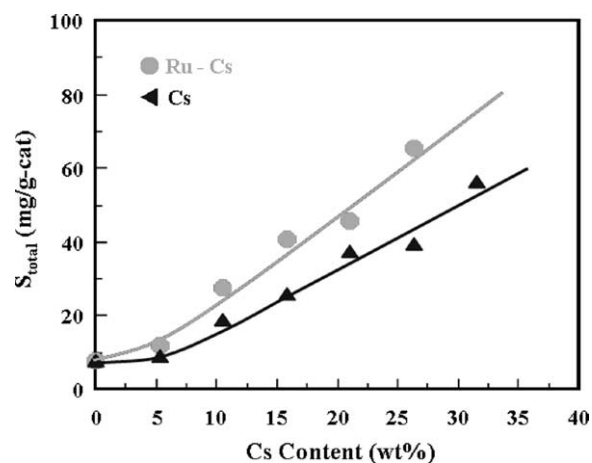
Fig. 8. Change in total sulfur with cesium content (Ru–Cs/Al$_2$O$_3$, Cs/Al$_2$O$_3$).

3.2. Effect of Ru/Cs ratio on the Ru–Cs catalyst sulfidation state

We have already reported that a significant increase in the catalytic activity is observed when the Cs/Ru ratio increases [25]. We decided therefore to perform tracer experiments on solids prepared with various Cs/Ru ratios. Results are summarized in Figs. 9 and 10, and Table 3. The DBT conversion and S_{total} changed only a little when the Cs/Ru ratio increased from 0 to 1. However, a further Cs/Ru ratio increase led to an increase of S_{total} (Fig. 9). Using FTIR experiments, we have shown in a previous paper [25] that for Cs/Ru = 1, created Cs[HRu$_3$(CO)$_{11}$] species are destroyed during the impregnation stage. Indeed, HRu$_3$(CO)$_{12}$ species were detected on the surface of the catalysts, indicating that Cs reacted with the acid sites of the alumina. Therefore, in such a system, Ru-containing particles were isolated from the Cs-containing ones before the presulfidation stage and a synergetic effect was not observed. Indeed, DBT HDS activity of the solid prepared with Cs/Ru = 1 was almost the same as the one observed over the corresponding Cs-free catalyst. Results were different for higher loading of Cs

Fig. 9. Change in conversion and S_{total} with Cs/Ru (8 wt% Ru–Cs systems).
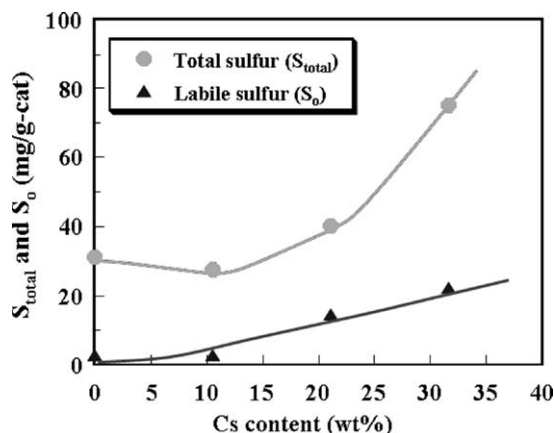
Fig. 10. Change in S_{total} and S_0 with Cs content in Ru–Cs/Al$_2$O$_3$ catalysts (Ru 8 wt%).

Table 3
Kinetic parameters on Ru–Cs/Al$_2$O$_3$

Ru:Cs	Conversion (%)	S_{total} (mg/g-cat)	S_0 (mg/g-cat)	S_{0A} (mg/g-cat)
1:0	50	31.4 (RuS$_{1.27}$)	2.2	9.2 (RuS$_{0.36}$)
1:1	54	27.5 (RuS$_{1.11}$)	2.8	18.3 (RuS$_{0.72}$)
1:2	94	40.4 (RuS$_{1.63}$)	14.7	38.5 (RuS$_{1.52}$)
1:3	97	75.1 (RuS$_{2.72}$)	22.0	39.3 (RuS$_{1.55}$)

Ru 8 wt%.

for which Cs–Ru interaction was preserved. Indeed, FTIR results show that the [HRu$_3$(CO)$_{11}$]$^-$ structure was present for Cs/Ru = 2, indicating that this ratio is enough to saturate alumina acid sites with Cs atoms, leaving a part of the prepared complexes intact on the alumina surface. While during the presulfidation stage the complex structure was broken, it is likely that Ru to Cs atom proximity was preserved. It is therefore reasonable to postulate that Ru–Cs was responsible for the increase in HDS activity and S_{total} observed in Fig. 9. For Cs/Ru = 3, FTIR analysis showed that anionic species were also maintained on the surface of the catalysts, but not in the [HRu$_3$(CO)$_{11}$]$^-$ form. Nevertheless, Cs–Ru interaction was preserved, which is linked with further increase in S_{total} observed in Fig. 9. Moreover, for Cs/Ru = 3, the observed value of S_{total} suggested that there was a lot of sulfur existing not only as RuS$_2$ but also as CsSH.

In addition, the amount of labile sulfur increased drastically for Ru/Cs > 1 (Fig. 10), i.e., when FTIR data suggest that the direct interaction between Cs and Ru species in the Cs[HRu$_3$(CO)$_{11}$] complex is preserved after impregnation. This suggests that Cs strengthens the Ru–S bond of the Ru sulfide species, which leads to an increase in S_0 and therefore to an increase in activity.

Further, the total sulfur amount accommodated on Cs/Al$_2$O$_3$ catalysts was compared with the one accommodated on Ru–Cs catalysts with various Cs/Ru ratios. Fig. 11 shows the variation of (S_{total}) for Ru–Cs and Cs catalysts. Except for Ru/Al$_2$O$_3$ catalyst (i.e., Cs free), S_{total} of
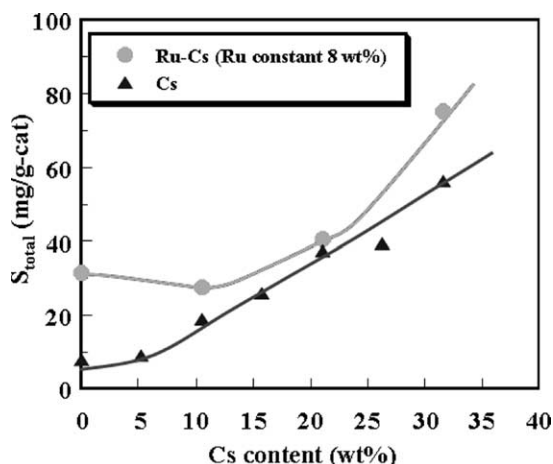

Fig. 11. Change in S_{total} with Cs content [Ru–Cs/Al$_2$O$_3$ (Ru 8 wt%, Cs/Ru = 0–3), Cs/Al$_2$O$_3$].

both Ru–Cs/Al$_2$O$_3$ and Cs/Al$_2$O$_3$ increased approximately linearly with increasing Cs content. It was confirmed that a considerable amount of S_{total} in Ru–Cs/Al$_2$O$_3$ catalysts was related to the presence of Cs.

In brief, a direct interaction between Cs and Ru was responsible for an increase in S_0, inducing an increase in the observed HDS activity, and Cs presence induced an increase in S_{total}, supposedly by the creation of Cs–S bond-containing species.

3.3. Comparison of the amount of labile sulfur on the presulfided catalysts and on the working catalysts ([^{35}S]DBT HDS reaction)

In part 1 labile sulfur quantity created during the presulfidation stage was found to be very low, which could not explain the high activity of the catalytic system. Therefore, the amount of labile sulfur formed under working HDS conditions was checked. This amount (S_{0A}) evaluated in HDS of [^{35}S]DBT [49] was found to be very high when compared to S_0 observed after presulfiding reaction with [^{35}S]H$_2$S.

Fig. 12 shows the change in the radioactivities of produced [^{35}S]H$_2$S and unreacted [^{35}S]DBT during the HDS reaction of [^{35}S]DBT. After the HDS of [^{32}S]DBT reached the steady state, the reaction solution of [^{32}S]DBT was replaced by that of [^{35}S]DBT. The radioactivity of unreacted [^{35}S]DBT in the outlet of the reactor increased immediately and reached a steady state. However, the radioactivity of produced [^{35}S]H$_2$S showed a delay to reach the steady state. This result indicates that the sulfur in DBT is not immediately released as hydrogen sulfide, but accommodated on the catalysts, as observed on conventional catalysts [42,59]. In order to determine the amount of labile sulfur, after the radioactivity of [^{35}S]H$_2$S reached the steady state, decalin only was fed into the reactor. The radioactivity of [^{35}S]DBT decreased immediately, while the radioactivity of [^{35}S]H$_2$S gradually decreased. After the radioactivity of released [^{35}S]H$_2$S reached a value of 0 dpm, a [^{32}S]DBT solu-
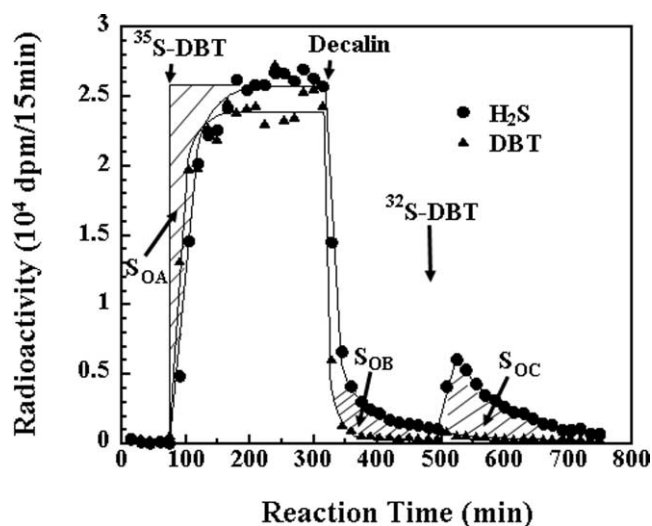
Fig. 12. Change in radioactivity of $[^{35}S]DBT$ and $[^{35}S]H_2S$.

Fig. 13. Effect of Ru content on DBT conversion and S_{total}.

tion was fed into the reactor. The ^{35}S accommodated on the catalyst during $[^{35}S]DBT$ HDS reaction was exchanged with ^{32}S released by $[^{32}S]DBT$ HDS and $[^{35}S]H_2S$ was detected again. When the $[^{32}S]DBT$ solution was introduced, the activities of the catalysts with high Ru contents decreased to about 70% of the original activity. This reflects the fact that since Ru sulfide is unstable under high H_2 pressure, sulfur in the catalyst reacted with hydrogen during the decalin introduction step (no sulfur was present in the feed) and was released as hydrogen sulfide (Ru reduction). Therefore, S_{0A} were evaluated by the addition of S_{0B} (sulfur released by reduction when no sulfur is fed into the reactor) and S_{0C} (sulfur exchanged by $[^{32}S]DBT$ reaction) (see Fig. 12). Fig. 13 shows the changes in DBT conversion and S_{0A} with Ru content for catalysts with Cs/Ru = 1. Both values increased with increasing Ru content but conversion exhibited a slight decrease for Ru > 16%. From these results, it was suggested that Ru species are uniformly dispersed on the alumina at least up to 16 wt% Ru. S_{0A} variation was also determined for catalysts with different Cs/Ru ratios. S_{0A} of the latter are shown in Table 3, in which we reported also the corresponding S_0. While for Ru–Cs/Al$_2$O$_3$ catalysts with Cs/Ru = 1, S_{0A} given as the number of labile sulfur for 1 Ru atom was 0.51–0.75, it was 0.36–1.55 for the catalysts with Cs/Ru = 0–3 and 8 wt% Ru (Table 3).

We have shown before that S_0 (labile sulfur quantity on the presulfided catalyst) was low on the catalysts, especially in the case of Cs/Ru = 1, meaning that for low Cs/Ru ratios, labile sulfur was hardly formed before the HDS reaction began. To compare the catalytic system presented in this study with other systems, we also listed in Table 4 presulfidation results reported by our group for Mo, Pt, and Pd systems. It is remarkable that for more conventional catalysts, the number of labile sulfur is high after the presulfidation (high value of S_0), while for Ru–Cs catalysts this number is low and labile sulfur is created only under the working conditions. Finally, taking into account the
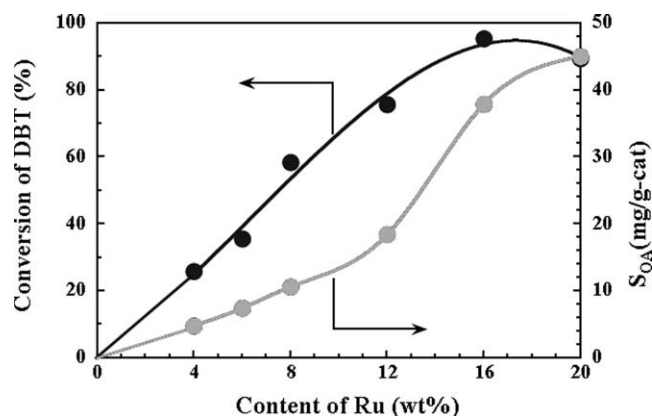
experimental results and models previously developed for other catalysts, we proposed a structure for Ru–Cs catalysts in Fig. 14. For the catalysts with Cs/Ru ratios equal to 2 or 3 (Fig. 14a), Cs and Ru interaction (preserved as shown by FTIR experiments) strengthens the Ru–S bond. Since the dispersion of Ru was expected to be very high (linear increase of the HDS activity up to 16 wt% Ru), a MoS$_2$-like single-layer structure was applied [57,58]. Four kinds of sulfur, S^a, S^b, S^c, and S^d can exist in the proposed structure. The S^a emerging from the catalyst surface might be easy to remove while the S^b in contact with alumina and covered with Ru might not be easy to be involved into a reaction as they are difficult to approach. S^c and S^d can be considered to be of a type between S^a and S^b. Therefore, in the best case 75% of the accommodated sulfur can move, which is consistent with the experimental results. For the catalysts with Cs/Ru = 1, impregnated complex is destroyed (FTIR results), and the structure of the catalysts is very likely to be as the one presented in Fig. 14b. Indeed, all the introduced Cs is consumed to neutralize the alumina acid sites. Moreover, S^b and S^c cannot move because of the steric hindrance but also because the Ru–Cs bond is not destabilized by the direct interaction with Cs species.

Table 4
Evaluation of sulfidation state on various catalysts using ^{35}S pulse tracer method

Catalyst	Sulfidation state of metal sulfide	S_0, S_{0A}^*/S_{total}
Ru–Cs/Al$_2$O$_3$[a]	RuS$_{0.91–1.11}$	6–10%
Ru–Cs/Al$_2$O$_3$[b]	RuS$_{1.43–1.69}$	34–48%*
Ru–Cs/Al$_2$O$_3$[c]	RuS$_{1.11–2.72}$	7–36%
Ru–Cs/Al$_2$O$_3$[d]	RuS$_{1.54–3.40}$	23–59%*
Cs/Al$_2$O$_3$	CsS$_{0.62–0.74}$	–
Mo/Al$_2$O$_3$	MoS$_2$	< 75% in MoS$_2$
CoMo/Al$_2$O$_3$	CoS MoS$_2$	< 60% in MoS$_2$
NiMo/Al$_2$O$_3$	NiS MoS$_2$	< 40% in MoS$_2$
Pt–Pd/Al$_2$O$_3$	PtS$_{0.25}$ PdS$_{0.25}$	100%

[a] After presulfiding (Ru 4–20 wt%, Cs/Ru = 1).
[b] During HDS (Ru 4–20 wt%, Cs/Ru = 1).
[c] After presulfiding (Ru 8 wt%, Cs/Ru = 0–3).
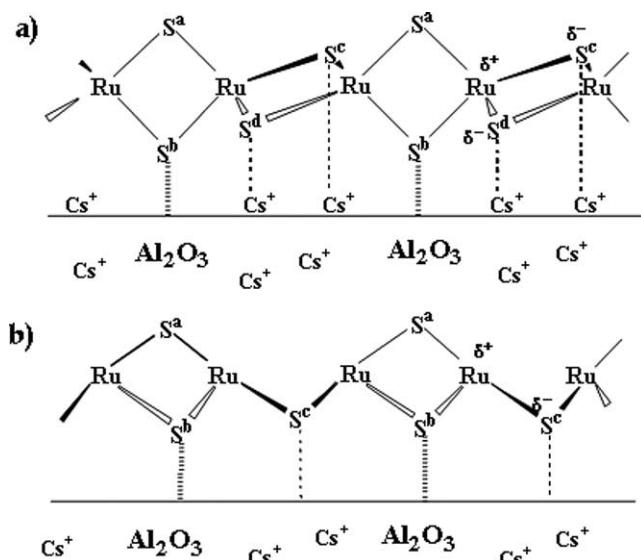[d] During HDS (Ru 8 wt%, Cs/Ru = 0–3).

Fig. 14. Sulfided Ru–Cs/Al$_2$O$_3$ catalysts structure. (a) Proposed structure for Cs/Ru = 2–3. (b) Proposed structure for Cs/Ru = 1.

Only S^a might be easy to remove and that is the explanation why the observed numbers of labile sulfur as well as the total number of accommodated sulfur were low. Fig. 15 shows the DBT hydrodesulfurization reaction mechanism over proposed catalyst structure in Fig. 14. First, DBT is adsorbed on the anion vacancy of the A structure and B state is formed. Then, DBT is desulfurized, one S atom remains on the active phase, and the structure C is formed. Furthermore, C reacts with H$_2$ to form E through D (H$_2$S desorption). For high Cs contents, the Ru–S bond is rather strong and therefore the catalyst steady state is likely to be B. Sulfur exchange proceeds in a manner like the one presented on Fig. 15 and when all of the labile sulfur is labeled by ^{35}S the quantitative analysis of labile sulfur becomes possible under the operating conditions.

In the case of Mo-based catalysts, Mo is sulfided up to MoS$_2$, and Co or Ni promoters are approximately in the CoS

and NiS forms, respectively [56,59]. Therefore, if we replace Ru by Mo in Fig. 15, steady state is C, where vacancies are not present. On the other hand, Pt and Pd catalysts were found to be in intermediate sulfidation states (PtS$_{0.25}$ and PdS$_{0.25}$) under the operating condition [52]. When Ru is replaced by Pt or Pd in Fig. 15, the structure of the Pt or Pd catalyst may be close to that of A or E. Under the reaction conditions Pt or Pd catalysts can exchange a lot of sulfur, as the amount of labile sulfur was found to be 100% (see Table 4). From these results, it is suggested that Ru catalysts have a medium sulfidation state between the one of Mo catalysts and the one of Pt or Pd catalysts.

4. Conclusions

1. During [^{35}S]DBT HDS reaction over Ru–Cs/Al$_2$O$_3$ catalysts, it was observed that the DBT conversion and labile sulfur amount (S_{0A}) increased with increasing Ru content. S_{0A} corresponded to 0.51–0.75 atom of S for 1 atom of Ru.

2. After Ru–Cs/Al$_2$O$_3$ catalysts presulfidation using [^{35}S] H$_2$S, the conversion of DBT and the amount of total sulfur (S_{total}) increased with increasing Ru content. S_{total} corresponded to 0.91–1.11 atom of S for 1 atom of Ru.

3. [^{35}S]H$_2$S Cs/Al$_2$O$_3$ catalysts [^{35}S]H$_2$S presulfidation experiments showed that the amount of total sulfur (S_{total}) increased with increasing Cs content. S_{total} corresponded to a CsS$_{0.62–0.74}$ formulation, and incorporated S quantity represented 70–80% of that incorporated on the corresponding Ru–Cs catalysts.

4. The amount of labile sulfur (S_0) formed after presulfidation of Ru–Cs/Al$_2$O$_3$ catalysts using [^{35}S]H$_2$S was much smaller than S_{total} or S_{0A}, indicating that the labile sulfur is difficult to form over the Ru–Cs/Al$_2$O$_3$ catalysts during the presulfidation stage.
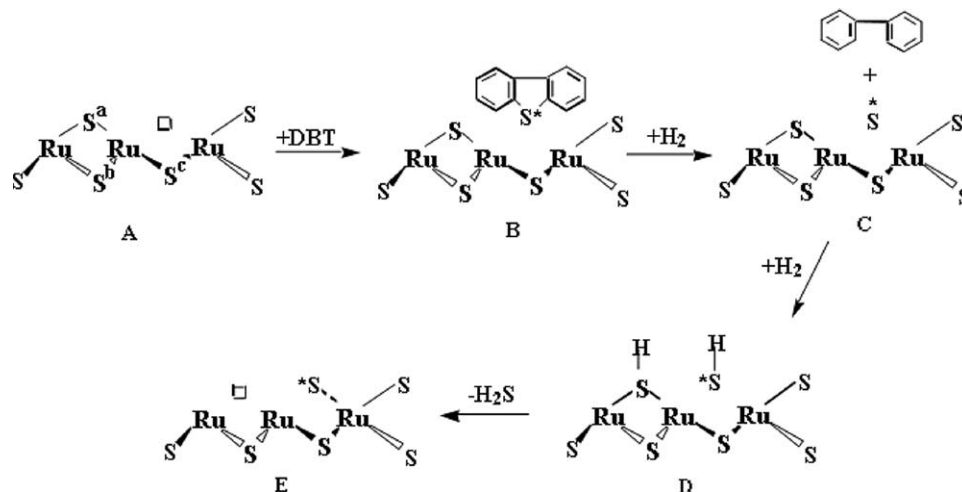

Fig. 15. DBT HDS reaction mechanism over sulfided Ru–Cs/Al$_2$O$_3$ catalysts.

5. The amount of labile sulfur (S_{0A}) observed during [^{35}S]DBT HDS as well as the conversion remarkably increased with increasing Cs/Ru (keeping Ru loading as a constant). S_{0A} corresponded to 0.36–1.55 atom of S for 1 atom of Ru.

6. Ru–Cs/Al$_2$O$_3$ catalyst [^{35}S]H$_2$S presulfidation experiments showed that the DBT conversion and the amount of total sulfur (S_{total}) remarkably increased with increasing Cs/Ru ratio. After presulfidation, S_{total} corresponded to 1.11–2.72 atom of S for 1 atom of Ru.

7. Taking into account various experimental results, a model proposing two Ru–Cs catalysts structures corresponding to two Cs/Ru domains was proposed. The DBT HDS mechanism of this model was discussed and compared with the one developed for Mo, Pd, and Pt catalysts.

The results showed that the sulfidation state and the mobility of sulfur over Ru catalysts greatly changes depending on the reaction conditions and suggested that the Ru catalysts have unique properties, different from the ones observed over Mo, Pt, or Pd catalysts.

Acknowledgments

References

[1] T. Kabe, A. Ishihara, W. Qian, Hydrodesulfurization and Hydrodenitrogenation, Kodansha Scientific, Wiley–VCH, Tokyo, 1999.
[2] M. Vrinat, M. Lacroix, M. Breysse, L. Mosoni, M. Roubin, Catal. Lett. 3 (1989) 405.
[3] A.P. Raje, S.-J. Liaw, B.H. Davis, Appl. Catal. 150 (1997) 297.
[4] A.P. Raje, S.-J. Liaw, R. Srinivasan, B.H. Davis, Appl. Catal. 150 (1997) 319.
[5] T.A. Pecoraro, R.R. Chianelli, J. Catal. 67 (1981) 430.
[6] M. Lacroix, N. Boutarfa, C. Guillard, M. Vrinat, M. Breysse, J. Catal. 120 (1989) 473.
[7] J. Shabtai, N.K. Nag, F.E. Massoth, J. Catal. 104 (1987) 413.
[8] J.A. De Los Reyes, M. Vrinat, C. Geantet, M. Breysse, Catal. Today 10 (1991) 645.
[9] K. Lu, Y.J. Kuo, B.J. Tatarchuk, J. Catal. 116 (1989) 373.
[10] A. Ishihara, M. Nomura, T. Kabe, J. Catal. 150 (1994) 212.
[11] M.J. Ledoux, O. Michaux, G. Agostini, P. Panissod, J. Catal. 102 (1986) 275.
[12] J.P.R. Vissers, C.K. Groot, E.M. Van Oers, V.H.J. de Beer, R. Prins, Bull. Soc. Chim. Belg. 93 (1984) 813.
[13] S. Eijsbouts, V.H.J. de Beer, R. Prins, J. Catal. 109 (1991) 217.
[14] T.G. Harvey, T.W. Matheson, J. Catal. 101 (1986) 253.
[15] J.L. Lamberton, M. Cattenot, V. Kougionas, M. Mhaouer, J.L. Portefaix, M. Breysse, G. Pérot, in: G.F. Froment, B. Delmon, P. Grange (Eds.), Hydrotreatment and Hydrocracking Oil Fractions, Elsevier, Amsterdam, 1997, p. 529.
[16] J.L. Zotin, M. Cattenot, J.L. Portefaix, M. Breysse, Bull. Soc. Chim. Belg. 104 (1995) 213.
[17] M. Breysse, M. Cattenot, V. Kougionas, J.C. Lavalley, F. Mauge, J.L. Portefaix, J.L. Zotin, J. Catal. 168 (1997) 143.
[18] S.-J. Liaw, R. Lin, A. Raje, B.H. Davis, Am. Chem. Soc. Dir. Petrol. Chem. 39 (1994) 636.
[19] M. Wojciechowska, M. Pietrowski, S. Lomnicki, Chem. Commun. (1999) 463.
[20] R. Navarro, B. Pawelec, J.L.G. Fierro, P.T. Vasudevan, Appl. Catal. A 148 (1996) 23.
[21] A. Maezawa, M. Kitamura, K. Wakamoto, Y. Okamoto, T. Imanaka, Chem. Expression 3 (1988) 1.
[22] Y. Okamoto, M. Odawara, H. Onimatsu, T. Imanaka, Ind. Eng. Chem. Res. 34 (1995) 3703.
[23] A. Ishihara, M. Nomura, T. Kabe, J. Jpn. Petrol. Inst. 37 (3) (1994) 300.
[24] A. Ishihara, M. Nomura, T. Kabe, Chem. Lett. (1992) 2285.
[25] A. Ishihara, M. Nomura, N. Takahama, K. Hamaguchi, T. Kabe, J. Jpn. Petrol. Inst. 39 (1996) 211.
[26] A. Ishihara, M. Nomura, K. Shirouchi, T. Kabe, J. Jpn. Petrol. Inst. 39 (1996) 403.
[27] A. Ishihara, K. Hamaguchi, T. Kabe, J. Jpn. Petrol. Inst. 40 (1997) 516.
[28] S. Yamada, W. Qian, A. Ishihara, G. Wang, L. Li, T. Kabe, J. Jpn. Petrol. Inst. 44 (2001) 217.
[29] W. Qian, S. Yamada, A. Ishihara, M. Ichinoseki, T. Kabe, J. Jpn. Petrol. Inst. 44 (2001) 225.
[30] C.G. Gachet, E. Dhainaut, L. De Mourgues, J.P. Candy, P. Fouilloux, Bull. Soc. Chim. Belg. 90 (1981) 1279.
[31] G.V. Isagulyants, A.A. Greish, V.M. Kogan, G.M. V'unova, G.V. Antoshin, Kinet. Catal. 28 (1987) 550.
[32] G.V. Isagulyants, A.A. Greish, V.M. Kogan, Kinet. Catal. 28 (1987) 220.
[33] G.V. Isagulyants, A.A. Greish, V.M. Kogan, Kinet. Catal. 28 (1987) 555.
[34] G.V. Isagulyants, A.A. Greish, V.M. Kogan, in: M.J. Pjilips, M. Ternan (Eds.), Proceedings of the 9th International Congress on Catalysis, Calgary, Ottawa, Canada, Vol. 1, 1988, p. 35.
[35] G.V. Isagulyants, A.A. Greish, V.M. Kogan, Catal. Lett. 6 (1990) 157.
[36] M. Dobrovolszky, K. Matusek, Z. Paal, P. Tetenyi, J. Chem. Soc., Faraday Trans. 89 (1993) 3137.
[37] V.M. Kogan, N.T. Dung, V.I. Yakerson, Bull. Soc. Chim. Belg. 104 (1995) 303.
[38] M. Dobrovolszky, Z. Paal, P. Tetenyi, Appl. Catal. 142 (1996) 159.
[39] V.M. Kogan, N.M. Parfenova, in: G.F. Froment, B. Delmon, P. Grange (Eds.), Hydrotreating and Hydrocracking of Oil Fractions, Elsevier, Amsterdam, 1997, p. 449.
[40] V.M. Kogan, in: T. Weber, R. Prins, R. van Santen (Eds.), Transition Metal Sulfides: Chemistry and Catalysis, High Technology, in: NATO ASI Series 3, Vol. 60, Kluwer Academic, Dordrecht, 1998, p. 235.
[41] V.M. Kogan, N.N. Rozhdestvenskaya, I.K. Korshevets, Appl. Catal. A: Gen. 234 (2002) 207.
[42] T. Kabe, W. Qian, A. Ishihara, J. Phys. Chem. 98 (1994) 3912.
[43] A. Ishihara, M. Yamaguchi, H. Godo, W. Qian, T. Kabe, Chem. Lett. (1996) 743.
[44] W. Qian, A. Ishihara, Y. Okoshi, W. Nakagami, M. Godo, T. Kabe, J. Chem. Soc., Faraday Trans. 93 (1997) 4395.
[45] A. Ishihara, M. Yamaguchi, H. Godo, W. Qian, M. Godo, T. Kabe, J. Jpn. Petrol. Inst. 41 (1998) 51.
[46] T. Kabe, A. Ishihara, W. Qian, M. Godo, Catal. Today 45 (1998) 285.
[47] W. Qian, Y. Yoda, Y. Hirai, A. Ishihara, T. Kabe, Appl. Catal. A: Gen. 184 (1999) 81.
[48] T. Kabe, W. Qian, A. Funato, Y. Okoshi, A. Ishihara, Phys. Chem. Chem. Phys. 1 (1999) 921.
[49] A. Ishihara, H. Godo, R. Kanamori, W. Qian, T. Kabe, Appl. Catal. A: Gen. 182 (1999) 345.
[50] T. Kabe, A. Ishihara, W. Qian, A. Funato, T. Kawano, React. Kinet. Catal. Lett. 68 (1999) 69.

[51] W. Qian, A. Ishihara, Y. Aoyama, T. Kabe, Appl. Catal. A: Gen. 196 (2000) 103.

[52] T. Kabe, W. Qian, Y. Hirai, L. Li, A. Ishihara, J. Catal. 190 (2000) 191.

[53] A. Ishihara, W. Qian, T. Kabe, J. Jpn. Petrol. Inst. 44 (2001) 80.

[54] T. Kabe, W. Qian, K. Tanihata, A. Ishihara, M. Godo, J. Chem. Soc., Faraday Trans. 93 (1997) 3709.

[55] E.P. Barrett, L.G. Joyner, P.P. Halenda, J. Am. Chem. Soc. 73 (1951) 373.

[56] T. Kabe, W. Qian, S. Ogawa, A. Ishihara, J. Catal. 143 (1993) 239.

[57] N.-Y. Topsøe, H. Topsøe, J. Catal. 139 (1993) 631.

[58] N.-Y. Topsøe, H. Topsøe, J. Catal. 139 (1993) 641.

[59] T. Kabe, W. Qian, A. Ishihara, J. Catal. 149 (1994) 171.